Shear Strength of Reinforced Concrete Shear Walls under Eccentric Tensile Axial Force

SHEAR STRENGTH OF REINFORCED CONCRETE SHEAR WALLS UNDER ECCENTRIC TENSILE AXIAL FORCE

Mitsuo MIZOGUCHI*1, Yasuyuki ARAI*1 and Koji HOSOYA*2

ABSTRACT

Six reinforced concrete shear wall models were built and tested to investigate effects of cyclic lateral loading and an eccentric tensile axial force on their shear strength behavior. The following are confirmed from this test result. When the elongation at the bottom of the boundary column on the compression side for a lateral force is small, the shear strength of shear walls subjected to a tensile axial force at the boundary column can be evaluated by conventional shear strength equations, regardless of cyclic lateral loading and the eccentric tensile axial force. However, when this elongation of the boundary column increases, the test maximum value is much lower than the value calculated from conventional equations.

KEYWORDS: reinforced concrete, shear wall, eccentricity, tensile axial force, shear strength

1. INTRODUCTION

At the first story of structural walls within high-rise buildings, it is considered that the boundary columns on the compression side for a lateral force may suffer a large tensile axial force generated by the overturning moment effect of the orthogonal direction because seismic forces could be applied from any direction. As well as the walls within these high-rise buildings, walls on the tension side of a non-planar wall like an L-shaped wall and a coupled shear wall with coupling beams may be subjected to a tensile axial force at the boundary column on the compression side for a lateral force. In our previous report [1], the lateral monotonically increasing loading test of shear walls in which a tensile axial force is applied to the boundary column on the compression side for a lateral force was carried out, and shear behavior of these walls was examined. According to this test result, the test values of strength agreed almost with the calculated values by the shear strength equation [3] using actual axial negative stress. Therefore, it was apparent that this equation could be used as the shear strength equation of the walls subjected to an eccentric tensile axial force. In this paper, the lateral cyclic loading test of six shear wall models which are subjected to a tensile axial force to the boundary column on the compression side for a lateral force is carried out, and then, the shear strength of these walls is examined.

2. EXPERIMENTAL PROGRAM

2.1 TEST SPECIMENS

A total of six I-shaped walls were tested to failure. All specimens had two boundary columns with a 15 cm

*1 Department of civil Engineering and Architecture, Muroran Institute of Technology
*2 Graduate Student, Muroran Institute of Technology

Table 1 Specimens and Bar Arrangements

Specimens	Thickness of Wall Panel t (mm)	Overall Length of Section D (mm)	Shear Reinforcement for Wall		Shear Reinforcement for Column		Calculated Strength at Designed Specimen(kN)			
			Bar Arrangement	Ratio Ps(%)*	Bar Arrangement	Ratio Pw(%)	Loading Direction	P	Bending Strength	Shear Strength
I-L65T1	50	1700	4φ@100	0.25	4φ@50	0.33	±	0	324	267
I-L65T2	49	1700	4φ@100	0.25	4φ@50	0.33	+	219	328	248
							-	-219	594	285
I-L65T3	49	1700	4φ@100	0.25	4φ@50	0.33	+	219	328	248
							-	110	185	245
I-H65T3	49	1700	4φ@50	0.51	4φ@50	0.33	+	226	345	268
							-	113	198	266
I-L63T3	46	1700	4φ@100	0.27	4φ@30	0.55	+	219	328	248
							-	110	185	245
IS-L65T3	52	1500	4φ@100	0.24	4φ@50	0.33	+	217	288	228
							-	109	162	214

* Ratio to Actual Thickness of Wall Panel

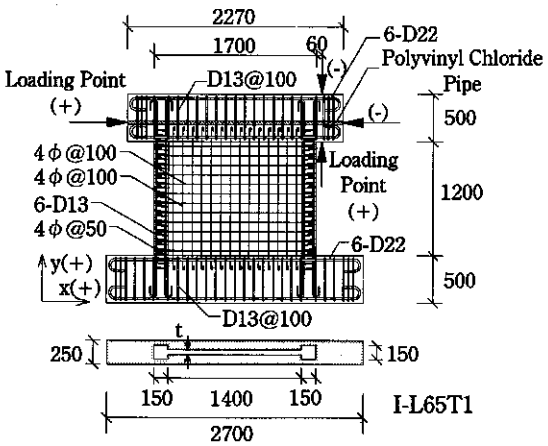

Fig. 1 Details of Specimen (mm)

Table 2 Strength Equations

Bending Yielding Strength[2]

$$My = 0.8at \cdot \sigma y \cdot D + 0.2aw \cdot \sigma wy \cdot D + 0.5N \cdot D\left(1 - \frac{N}{B \cdot D \cdot Fc}\right) \quad \cdots(1)$$

Bending Strength[3]

$$Mbu = 0.9at \cdot \sigma y \cdot D + 0.4aw \cdot \sigma wy \cdot D + 0.5N \cdot D\left(1 - \frac{N}{Bc \cdot D \cdot Fc}\right) \quad \cdots(2)$$

Shear Strength[3] (Unit : kgf, cm)

$$Qsu = \left\{\frac{0.068 pte^{0.23}(Fc + 180)}{\sqrt{M/(Q \cdot D)} + 0.12} + 2.7\sqrt{\sigma wh \cdot pwh} + 0.1\sigma_0\right\} be \cdot j \quad \cdots(3)$$

Shear Strength ("AIJ Design Equation"[4])

$$Vu = tw \cdot lwb \cdot ps \cdot \sigma sy \cdot \cot\phi + \tan\theta(1 - \beta) tw \cdot lwa \cdot \nu \cdot \sigma_B / 2 \quad \cdots(4)$$

here $\tan\theta = \sqrt{(hw/lwa)^2 + 1} - hw/lwa$

$\nu = 0.7 - \sigma_B / 200$

hw : height of loading point from hooting beam

Please refer to references for each symbol.

Table 3 Properties of Concrete

Specimens	Compressive Strength (N/mm^2)	Tensile Strength (N/mm^2)	Secant Modulus of Elasticity (N/mm^2)
I-L65T1	23.7	1.85	19700
I-L65T2	22.8	1.80	19800
I-L65T3	23.5	1.93	21300
I-H65T3	23.5	1.64	22000
I-L63T3	22.4	1.79	21200
IS-L65T3	23.4	1.92	21700

Table 4 Properties of Reinforcement

Size	Cross-section Area (cm^2)	Yielding Strength (N/mm^2)	Tensile Strength (N/mm^2)	Elongation Percentage (%)
D22	3.87	393	592	24
D13	1.267	370	527	27
4ϕ	0.124	202	300	51

square section, and the clear height of the wall was 120 cm. The overall length of the section of the wall was 170 cm in five specimens and 150 cm in the other specimen. Though the thickness of the wall panel was designed with a thickness of 5 cm, actual dimensions of the test specimens varied as shown in Table 1. Main reinforcement bars 13 mm in diameter were used in each column. Square spiral hoops made of wire 4 mm in diameter with two kinds of spacing (5 cm and 3 cm) were used in the columns. Reinforcement wire of 4 mm in diameter was used in each wall panel with two kinds of spacing (10 cm and 5 cm). Details of the reinforcement for test specimens are shown in Table 1. As an example, bar arrangements and dimensions of I-L65T1 are shown in Fig. 1. Though the dimension and the reinforcement of I-L65T1, I-L65T2 and I-L65T3 were the same, these three specimens were tested under different axial forces that were given by P (upward direction is positive) shown in Table 1 at the maximum lateral load. All specimens were designed to fail in shear in the positive loading under an eccentric tensile axial force. The calculated values of the bending and shear strength at the design stage are also shown in Table 1. This bending strength is the value calculated considering both the moment obtained by Equation (2) [3] in Table 2 at the bottom of the wall and the bending moment caused by the eccentric tensile axial force P at the top of the wall. This shear strength is the calculated value given by Equation (3) [3] shown in Table 2. Normal concrete with a maximum aggregate size of 10 mm and specified design strength $21N/mm^2$ was used for the test specimens. All specimens were horizontally cast in forms. The material properties are given in Tables 3 and 4.

2.2 TEST PROCEDURE AND INSTRUMENTATION

As shown in Fig. 2, the lateral and longitudinal forces were applied by two hydraulic actuators named as ① and ②, respectively. The lateral load at the top of the wall was applied by actuator ① that produced the cyclic gradual increment of a lateral deflection. To produce a negative lateral deflection, a steel loading rod through a polyvinyl chloride pipe that was placed in the loading beam was adjusted. The reversed deflection increments were at rotation angles of 1×10^{-3}, 2×10^{-3}, 4×10^{-3}, 6×10^{-3} and 10×10^{-3} radians in the x-direction. In I-L63T3 and IS-L65T3, 4×10^{-3}

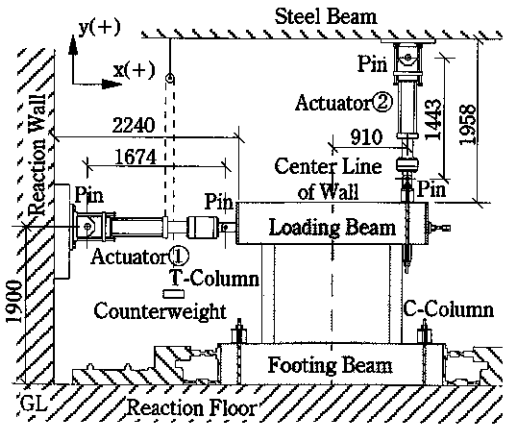

Fig. 2 Loading Apparatus (mm)

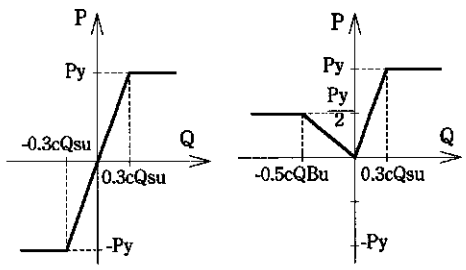

(a) I-L65T2

(b) I-L65T3, I-H65T3, I-L63T3, IS-L65T3

Fig. 3 Settings of Axial Force

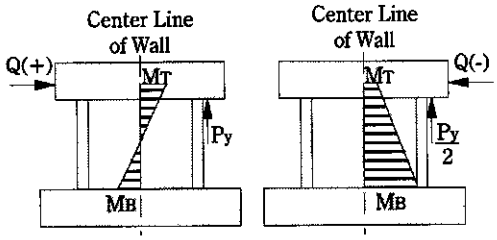

Fig. 4 Moment Distributions

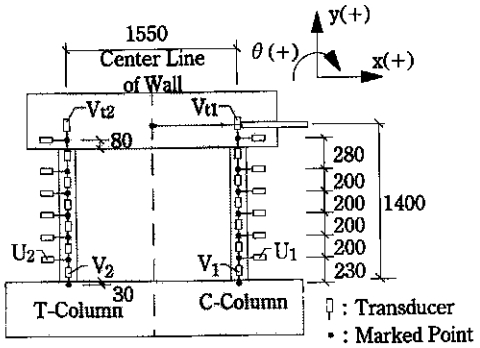

Fig. 5 Measuring Points of Displacement (mm)

radian was omitted. In I-L65T2, the negative deflection of each cycle was limited at rotation angle of 1×10^{-3} radian in order to make the specimen fail in shear in the positive loading. In four specimens except I-L65T1 and I-L65T2, the first lateral load was applied to the negative direction. The longitudinal force was applied at the loading point on the loading beam. As shown in Fig. 3, the longitudinal force was given as a function of the lateral load Q. The longitudinal force was applied so that C-column on the compression side for a lateral force may suffer a large tensile axial force in the positive loading and the wall may not fail in shear in the negative loading. Py in Fig. 3 was the calculated value assuming that the moment MT at the top of the wall as shown in Fig. 4(a) was equal to bending yield moment My (N=-Py) given by Equation (1) [2] in Table 2. $_cQ_{SU}$ and $_cQ_{BU}$ are the calculated values of the shear and bending strengths and are shown in Table 1. The lateral displacements of a loading beam and the longitudinal displacements at the top of each column were measured with respect to the footing beam, as shown in Fig. 5. The elongations and the lateral displacements of each column were measured at marked points dividing the wall height into six portions. The strains in the main reinforcing bar of columns were also measured by wire strain gauges.

3. TEST RESULTS AND DISCUSSION

3.1 FRACTURE PROCESSES

Figure 6 gives the cracking patterns of walls after failure. The solid and broken lines in this figure show the

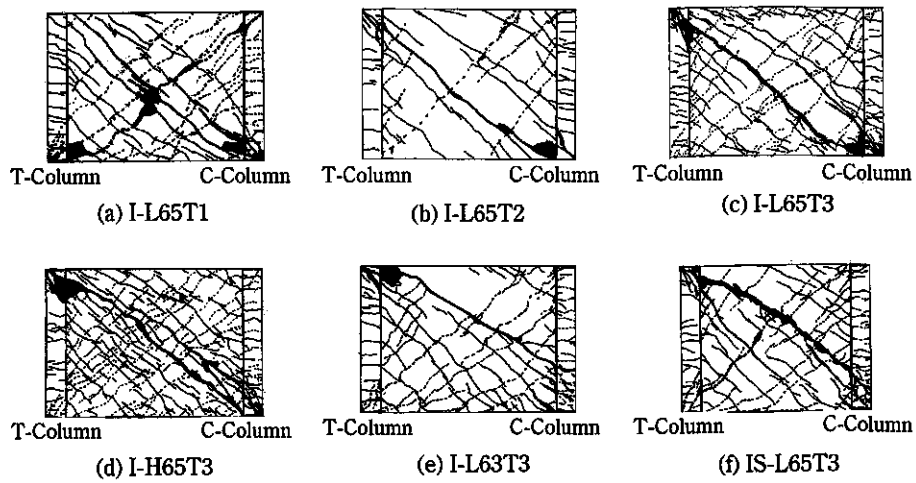

Fig. 6 Cracking Patterns

cracks that appeared during the positive and negative loading, respectively. In I-L65T1 without an axial force, diagonal cracks occurred under both positive and negative loading, and these cracks intersected at the wall panel. In the negative loading, the wall failed in shear when the width of diagonal cracks of the wall panel was widened and inclined cracks occurred at both boundary columns. In I-L65T2 subjected to the eccentric axial force, the tensile force in the positive loading and the compressive force in the negative loading, though the diagonal cracks occurred at the wall panel and these cracks intersected, the number of the cracks was less than that of I-L65T1. In the positive loading, the wall failed in shear when the shear cracks passed through both boundary columns, and the opening of diagonal cracks near the diagonal line was observed simultaneously. In four specimens, I-L65T3, I-H65T3, I-L63T3 and IS-L65T3, subjected to the eccentric tensile axial force under positive and negative loading, diagonal cracks occurred and these cracks intersected at the wall panel as I-L65T1. However, the number of the cracks of I-H65T3 with a large shear reinforcement ratio within a wall panel was more than that of the other specimens. In both I-L63T3 with a higher shear reinforcement ratio in the columns and IS-L65T3 with the short overall length of the section of the wall, diagonal cracks that occurred under positive loading slightly above the diagonal line of the wall had gentle inclinations. These four test specimens failed in shear under positive loading when the opening of inclined cracks at the boundary columns was observed and the width of the diagonal cracks shown by the bold line in Fig. 6 was widened simultaneously.

3.2 LOAD-DEFLECTION CURVES

Figure 7 shows the relationships between the lateral load, Qx, and the drift angle, Rx, at the top of the wall. Rx is defined as the lateral displacement of the loading beam divided by the height from the lateral loading point to the top of the footing beam. In I-L65T1 without an axial force, the main reinforcement at the bottom of T-column yielded, and little decrease in the load carrying capacity was observed after the maximum lateral load was reached under positive loading. However, after the maximum lateral load was reached, the load carrying capacity suddenly decreased due to the opening of both diagonal cracks of the wall panel and shear cracks of the columns just after the main reinforcement of C-column yielded under negative loading. In five specimens subjected to the eccentric tensile axial force under positive loading, I-L65T2, I-L65T3, I-H65T3, I-L63T3 and IS-L65T3, the decrease in the load carrying capacity was observed when the width of both diagonal cracks of the wall panel and shear cracks of the columns widened in the positive loading. In four specimens subjected to the eccentric tensile axial force under negative loading, I-L65T3, I-H65T3, I-L63T3 and IS-L65T3, the main reinforcement at the bottom of C-column yielded, and little decrease in the load carrying capacity was observed after the reinforcement yielded.

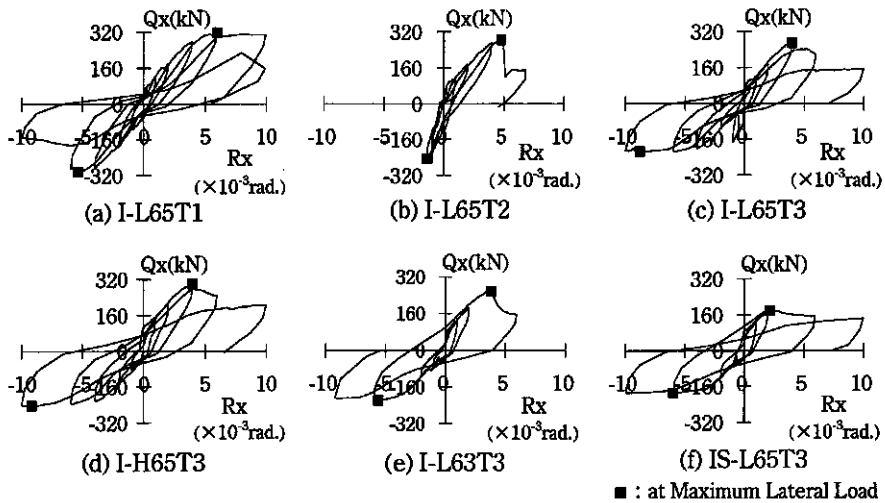

Fig. 7 Load-Deflection Curves

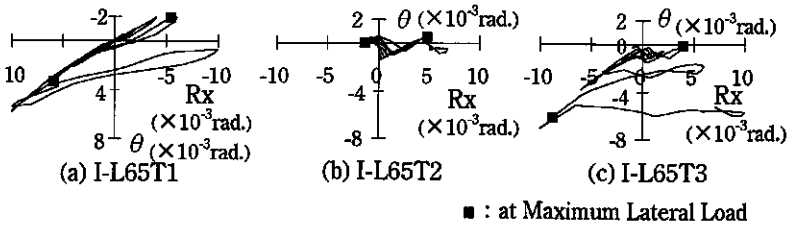

Fig. 8 Relationships between Rotation Angle and Deflection

3.3 ROTATIONAL ANGLE OF WALL TOP

Figure 8 shows the relationships between the rotational angle at the top of the wall, θ, and the drift angle, Rx, at the top of the wall. Only three specimens with the different eccentric axial forces are shown in this figure. The rotational angle, θ, is calculated from the measured values of two longitudinal transducers, V_{t1} and V_{t2}, shown in Fig. 5. In I-L65T1 without an axial force, though the rotation angle was almost proportional to the drift angle, the change ratio of the rotation angle to the drift angle decreased after the maximum load was reached under negative loading with shear failure. In I-L65T2 subjected to the eccentric axial force, the tensile force in the positive loading and the compressive force in the negative loading, the rotation angle at the positive maximum lateral load is small due to the eccentric axial force. In I-L65T3 subjected to the eccentric tensile axial force under positive and negative loading, the rotation angle that grew under negative loading was kept constant until the positive loading due to the effect of the eccentric tensile force. The other three specimens that were not shown here had almost the same relationship between the rotation angle and the drift angle as I-L65T3. Therefore, it is obvious that the proportion of the shear deformation to the lateral deformation increases when the boundary column on the compression side for a lateral force suffer the tensile axial force.

3.4 DEFORMATION OF COLUMN BOTTOM

Figure 9 gives the lateral load-lateral displacement relationships at the bottom of the column and the lateral load-longitudinal displacement (= elongation) relationships at the bottom of the column. This figure shows T-column of I-L65T1 and C-column of other five specimens that became the column on the compression side for the lateral force when the wall failed in shear. In this figure (a) I-L65T1, negative loading is plotted in the upper ordinate, because the loading direction that shear failure occurred was different from the other five specimens. The lateral displacements u_1, u_2 and the longitudinal displacements v_1, v_2 are values measured by transducers, U1, U2, V1 and V2, mounted at the bottom of the columns as shown in Fig. 5. In I-L65T1 without an axial force, the longitudinal displacement observed under positive loading was reduced to almost 0 mm in the negative loading. However, the longitudinal displacement remained when this displacement increased after the main reinforcement at the bottom of T-column yielded under positive loading. This residual displacement became the longitudinal displacement of the negative loading. In I-L65T2 subjected to the eccentric axial force, the tensile force in the positive loading and the compressive force under negative loading, the longitudinal displacement under negative loading was small due to the eccentric compressive force. The longitudinal displacement at the positive maximum load was smaller than that of I-L65T1. In four specimens, I-L65T3, I-H65T3, I-L63T3 and IS-L65T3, subjected to the eccentric tensile axial force under both positive and negative loading, the first loading was applied in the negative direction. These longitudinal displacements observed under negative loading were kept constant under positive loading. The longitudinal displacements of both I-L65T3 and I-H65T3 at the maximum load were slightly larger than that of I-L65T1. Since both I-L63T3 and IS-L65T3 reached the maximum load after the large longitudinal displacement was observed under negative loading, the displacements of these specimens were even larger than those of both I-L65T3 and I-H65T3. All the lateral displacements at the maximum load of the loading direction with shear failure were about 3 mm. Therefore, there was no difference of this displacement among all specimens as the longitudinal displacement, axial load, reinforcement within a wall panel and shear reinforcement of column changed. In all specimens, when the lateral displacement at the bottom of the column on the compression side grew to about 3 mm, an opening of the shear crack of the column was observed, and the wall failed in shear.

3.5 SHEAR STRENGTH

Table 5 lists the maximum test values, tQmax, and calculated values. In addition, the eccentric tensile force, P, and the drift angle, R, at the maximum lateral load are also shown in Table 5. The calculated value cQbu is the bending strength calculated considering both the moment caused by the eccentric tensile force P at the top of the wall and the moment obtained by Equation (2) [3] shown in Table 2 at the bottom of the wall. The calculated value cQsu is given by Equation (3) [3] shown in Table 2 using the actual axial negative stress σ_0 which occurs by the eccentric tensile force. Shear span M/Q is calculated from the bending moment distributions given by both the eccentric tensile force P and the test value of tQmax. The calculated value Vu is obtained from Equation (4) [4] shown in Table 2. The test values obtained in the negative loading of I-L65T1 and in the positive loading of other five specimens are discussed. These were given when the wall failed in shear. In the three specimens with the same bar arrangement and shape, the test value of I-L65T1 without an axial force is 303kN. The test values of I-L65T2 and I-L65T3 with an eccentric tensile force are about 10% smaller than I-L65T1 and they are 283kN and 271kN, respectively. Therefore, the test value lowers, when a tensile axial force is applied. Here, a test result is compared with a calculated value. In IS-L65T3 with the short overall length of the wall, the ratio of the test result to the calculated value cQsu is 0.73. However, in the other five specimens, this ratio ranges from 1.03 to 1.10 with an average of 1.06. These calculated values are similar to the test results as well as the case of the monotonous loading reported in previous report [1]. In IS-L65T3, the ratio of the test result to the calculated value Vu was 0.69. This ratio of the other five specimens ranges from 0.89 to 0.97 with an average of 0.94, and the test results are slightly smaller than calculated values. In IS-L65T3 with the short overall length of the wall, the both ratios are much smaller than the others. According to Fig. 9, in this specimen, the elongation at the bottom

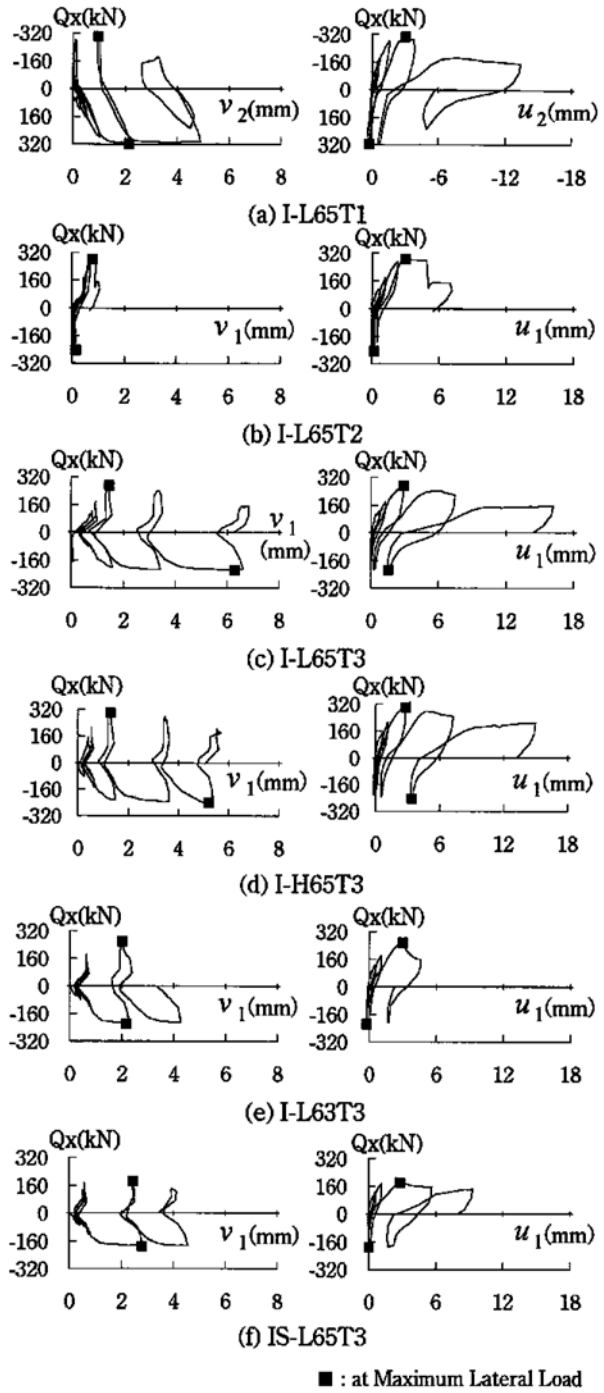

Fig. 9 Relationships between Load and Displacement of Column Bottom

Table 5 Ultimate Strength

Loading Direction	Specimens	Test Value				Calculated Value			Ratio			Failure Mode
		tQmax (kN)	P (kN)	σ_0* (N/mm^2)	R (10^{-3}rad.)	cQbu (kN)	cQsu (kN)	Vu (kN)	tQmax / cQbu	tQmax / cQsu	tQmax / Vu	
Positive	I-L65T1	316	0	0	5.98	324	284	312	0.98	1.11	1.01	Flexure
	I-L65T2	283	221	-1.95	4.78	329	258	296	0.86	1.10	0.96	Shear
	I-L65T3	271	222	-1.95	3.98	329	262	303	0.82	1.03	0.89	Shear
	I-H65T3	301	225	-1.98	3.99	346	282	325	0.87	1.07	0.93	Shear
	I-L63T3	257	220	-2.01	3.78	328	249	276	0.78	1.03	0.93	Shear
	IS-L65T3	181	218	-2.03	2.18	288	247	264	0.63	0.73	0.69	Shear
Negative	I-L65T1	-303	0	0	-5.38	324	284	312	0.94	1.07	0.97	Shear
	I-L65T2	(-245)	-222	1.95	-1.38	598	295	296	—	—	—	—
	I-L65T3	-215	108	-0.95	-8.78	187	263	303	1.15	0.82	0.71	Flexure
	I-H65T3	-243	110	-0.97	-9.19	202	285	325	1.20	0.85	0.75	Flexure
	I-L63T3	-218	108	-0.99	-5.58	187	249	276	1.17	0.88	0.79	Flexure
	IS-L65T3	-189	107	-1.00	-5.98	163	236	264	1.16	0.80	0.72	Flexure

* Plus Sign was put to Compression Stress

of the column on the compression side is larger than that of the other test specimens at the maximum load. All test specimens are almost equal in the lateral displacements at the bottom of the column on the compression side at shear failure. Therefore, it seems that the test result of IS-L65T3 becomes lower than calculated values because the lateral stiffness of the boundary column is drastically reduced as the elongation increases at the bottom of this column in comparison to the other specimens. The ratio of tQmax to cQbu ranges from 1.15 to 1.20 in the negative loading of four specimens subjected to the eccentric tensile axial force in the negative loading. tQmax is about 17% larger than cQbu.

4. CONCLUSIONS

Based on the test results of shear walls subjected to cyclic lateral loading and an eccentric tensile axial force, the following conclusions can be made. The shear strength can be estimated by the conventional shear strength equation, if the elongation at the bottom of the column on the compression side for a lateral force is small. However, if this elongation increases, the shear strength decreases and may become lower than the calculated value by the shear strength equation. It is necessary to continue investigation on the degree of this elongation at the bottom of the column on the compression side.

ACKNOWLEDGMENT

This investigation was supported by the 2000 Grant-in-Aid for Scientific Research, Ministry of Education, Science, Sports and Culture of Japan.

REFERENCES

(1) Mizoguchi, M., Arai, Y., Kuchiji, H., "Shear Behavior of Reinforced Concrete Shear Walls under Tensile Axial Force with Eccentricity," Transactions of the JCI, Vol.22, Feb. 2001, pp.369-376.

(2) Hirosawa, M., "Past Experimental Results on Reinforced Concrete Shear Walls and Analysis on them," Kenchiku Kenkyu Shiryo, No.6, Mar. 1975, pp.33-34.

(3) AIJ, "Ultimate Strength and Deformation Capacity of Buildings in Seismic Design (1990)," 1990, pp.401-403.

(4) AIJ, "Design Guidelines for Earthquake Resistant Reinforced Concrete Buildings Based on Inelastic Displacement Concept," 1999, pp.209-214.